

Conversion of cellulose to activated carbons for high-performance supercapacitors

E. Sermyagina^{1,*}, K. Murashko², D. Nevstrueva¹, A. Pihlajamäki¹ and E. Vakkilainen¹

¹LUT University, Energy Technology, Laboratory of Sustainable Energy Systems, Skinnarilankatu 34, FI53850 Lappeenranta, Finland

²University of Eastern Finland, Fine Particle and Aerosol Technology Laboratory, Yliopistonranta 1 C, FI70210 Kuopio, Finland

*Correspondence: ekaterina.sermyagina@lut.fi

Abstract. Biomass-derived activated carbons are promising materials that can be used in various applications. Current work investigates the possibilities of the cellulose-derived activated carbons in substituting the commercial alternatives for the supercapacitors' electrodes with high efficiency, stable performance and relatively low cost. Hydrothermal carbonization (HTC) followed by chemical activation with KOH is used to convert cellulose into highly porous activated carbons. The effect of HTC parameters on the material porosity development and electrochemical properties of the electrodes is evaluated with several variations of the residence time and the weight ratio between cellulose and water during the pretreatment. The analysis shows that intensification of the HTC process (longer residence time and higher water/cellulose ratio) results in increase of the surface area of both hydrochar samples and subsequent activated carbons: with the highest surface area for the sample produced after 2 h HTC treatment with water/cellulose ratio of 6/1 - 2,645 m² g⁻¹. As for the electrochemical analysis, the highest values of the specific capacitance are found for the samples produced from 2 h HTC treatment: 110.3 F g⁻¹ (water/cellulose ratio of 3/1) and 102.5 F g⁻¹ (water/cellulose ratio of 6/1). Additionally, it is noted that electrodes produced from the samples treated during 4 h have higher impedance at low operation frequency. The present study proves the possibility to substitute commercial activated carbons with cellulose-derived materials, the porosity of which can be tuned accordingly already during the pretreatment step.

Key words: cellulose, hydrothermal carbonization, activated carbon, electrodes, supercapacitors.

INTRODUCTION

Activated carbons (AC) present the carbonaceous materials with high specific surface areas and adjustable surface-containing functional groups (Kuzmenko et al., 2015). The beneficial features of AC make them highly widespread in various modern applications and technologies. Their versatile properties allow them to be efficiently applied as adsorbents: in applications including the removal of heavy metals, organic compounds and dyes, toxic substances and different impurities in water and in air (Rengaraj et al., 2002; Babel & Kurniawan, 2003; Jiang et al., 2003; Crini, 2006; Mohan & Pittman Jr., 2007). Another important area for the AC is the electrical energy storage

applications: carbonaceous materials are widely used for lithium-ion batteries and for supercapacitors due to physical and chemical stability and high conductivity, significant surface area and porosity (Pandolfo & Hollenkamp, 2006; Zhu et al., 2011).

The activated carbons can be produced by several activation methods: physical (thermal), chemical or physicochemical activation (a combination of both) (Hernández-Montoya et al., 2012; Kuzmenko et al., 2015). During thermal activation, the precursor is carbonized under an inert atmosphere, and the resulting carbon is subjected to a partial gasification with an oxidizing gas (air, steam, CO₂, etc.) at high temperature (800–1,100 °C). Within the chemical activation, the feedstock is mixed with a chemical compound, generally a dehydrating agent (H₃PO₄, H₂SO₄, HNO₃, NaOH, KOH or ZnCl₂), and the mixture is subsequently heated to the temperature between 400 and 800 °C in an inert atmosphere. As for the physicochemical activation, the process is carried out with changing the activation atmosphere of the chemical activation to a gasification atmosphere (e.g. steam) at higher temperatures (Hernández-Montoya et al., 2012). As a rule, the chemical activation produces AC with the highest specific surface area. Additionally, the chemical activation provides more intensive development of micropores and requires lower temperatures than physical activation (Khezami et al., 2005). At the same time, the applied chemical agents make the process corrosive and require additional washing step for the products (Lozano-Castelló et al., 2001).

The majority of the commercial AC are the fossil fuel-based. Relatively high production cost and environmental concerns about the consequences of the coal and oil utilization drive the attention to alternative feedstock to produce the activated carbons from cheaper, renewable and widely available precursors (Mohamad Nor et al., 2013). Considering the increasing energy demand in the world and the promotion of sustainable materials and processes in different industrial spheres, biomass-derived activated carbons are highly promising materials for the supercapacitors' electrodes with high efficiency, stable performance and relatively low cost (Hernández-Montoya et al., 2012; Kuzmenko et al., 2015; Mesfun et al., 2019).

Alternative sources for activated carbons

The specific surface area and porosity of the activated carbons are determined by the feedstock material and activation procedure (Jiang et al., 2003). Hydrothermal carbonization (HTC) presents an attractive pathway to convert the organic materials into carbonaceous precursors for AC production (Li et al., 2020). Thermal treatment of the feedstock in a mixture with water in temperature range of 150–350 °C under autogenous pressures converts biomass into highly functionalized carbon materials (Titirici et al., 2007; Titirici & Antonietti, 2010). The resulted coal-like product (hydrochar) obtains a rudimental porosity due to the depolymerization and decomposition of the structural components and the consequent release of such elements as hydrogen, oxygen and nitrogen in form of condensable and non-condensable gases and tars (Hernández-Montoya et al., 2012). The liquid products of the HTC process contain volatile fatty acids and furfurals, which can be then effectively used in other applications (Sun et al., 2019).

In order to optimize the activation process towards the required resulting properties, the comprehensive knowledge of chemical components' behaviour during both carbonization and activation steps is needed. Several researchers have been investigating the possibilities of producing functional carbonaceous products from the main lignocellulosic structural components: glucose (Khezami et al., 2005; Lee et al., 2016;

Yuan et al., 2019), starch (Sevilla et al., 2011; Cao et al., 2018), cellulose (Deng et al., 2013; Wang et al., 2017) and lignin (Saha et al., 2014; Zhang et al., 2019). Cellulose has a significant impact on the microporosity development of the activated carbons from lignocellulosic feedstock: da Silva Lacerda et al. (2015) reported the increase of the adsorption properties of the activated carbons with artificially increased cellulose content. Sevilla et al. (2011) investigated the impact of activation parameters (temperature and hydrochar/KOH ratio) on the AC from hydrothermally carbonized cellulose and other lignocellulosic compounds for the gas storage applications. It was proven that the pore characteristics can be adjusted by changing the activation conditions: the highest porosity for cellulose derived AC was developed at the activation temperature of 700 °C and the hydrochar/KOH weight ratio of 1/4. The results presented by Wei et al. (2011) demonstrated a high potential to convert hydrothermally carbonized lignocellulosic materials (cellulose, starch and wood) into high surface area supercapacitors. Other researchers investigated the impact HTC temperature. In the work of Falco et al. (2013), three temperatures were tested (180, 240 and 280 °C) for cellulose, glucose and rye straw, and the highest surface area and total pore volume values were found for AC produced from samples carbonized at 240 °C. At the same time, more research is needed to evaluate in detail the effect of carbonization step on the resulted product, i.e. how the process severity (time, temperature, feedstock/water ratio) affects the porosity of activated carbons.

Tuning the microporosity of the ACs is important for some energy and environmental related applications (e.g., natural gas and hydrogen storage, supercapacitors, volatile organic compounds removal), where advanced porous materials with tailored porosity (extremely high development of microporosity together with a narrow micropore size distribution) are required (Hartmann et al., 2020). Using supercapacitors as an energy storage device is attracting an increasing attention worldwide (Kim et al., 2019). In the previous paper (Murashko et al., 2017), the material preparation methodology for a natural cellulose-activated carbon composite material was developed and described. The flexible self-standing electrodes for electrical double layer capacitors (EDLCs) were produced from the commercially available activated carbon with cellulose as a binding material. The aim of the current study is to investigate the possibility of substituting the commercial AC with the activated carbon from the cellulose derived hydrochar. Above all, the effect of HTC reaction parameters on porous structure evolution during activation and, as a result, on electrochemical characteristics of the produced electrodes was evaluated.

MATERIALS AND METHODS

Materials

High-purity cellulose (quality 2100 type, degree of polymerization 780, α -cellulose content $\geq 93\%$) produced by Domsjö Fabriker AB from softwood was used as a carbon precursor and an electrode binder. The material was cut to pieces with dimensions around 5–10 mm on average for the HTC experiments and grinded at the Retsch PM100 planetary ball mill to the powder state for the electrode preparation. Potassium hydroxide pellets (Sigma-Aldrich) were used as an activation agent and were grinded in the agate mortar before the experiments. Ionic liquid (IL), 1-ethyl-3-methylimidazolium acetate, was acquired from BASF (Basionics™ BC01, CAS: 143314-17-4, assay > 98%) and

used as received in preparation of an electrode casting solution. Sulphuric acid from Merck (CAS: 7664-93-9, assay 95–97%) was used to prepare a 1 mol sulphuric acid aqueous electrolyte. Deionized water was used for electrolyte preparation, for all electrode samples (as a coagulant) and during storage of the samples.

Preparation of hydrochar materials

Hydrochars were prepared by hydrothermal carbonization in 1 l stainless steel tube batch reactor. For each run, the feedstock material was dispersed in water, stirred manually and then loaded into the reactor. Heating (at the rate of 2 °C min⁻¹) to the process was provided by the electrical heater and controlled with a PID controller. The reaction temperature was maintained at 250 °C for all HTC runs. In this work, the following reaction parameters were tested: the residence time of 2 and 4 h; water-to-cellulose weight ratios of 3:1 and 6:1. The resulting solid product was recovered by vacuum filtration using the Büchner funnel with a Whatman glass microfiber filter paper (grade GF/A). Hydrochar samples were subsequently dried overnight in the oven at a temperature of 105 ± 2 °C.

Hydrochar samples were named in accordance with the reaction parameters as HTC-*t*-*r*_{HTC}, where *t* denotes the reaction time, h, and *r*_{HTC} the unitless water/cellulose weight ratio.

Preparation of porous carbons

The hydrochar samples were chemically activated at 700 °C with KOH. Hydrochar was thoroughly mixed with the activating agent at impregnation ratio (KOH/ hydrochar) of 4:1 in an agate mortar. Powder mixture was then loaded into the reactor where it was heated to the activation temperature with the heating ramp rate of 3 °C min⁻¹ under nitrogen gas flow and hold at the target temperature for 1 h. Finally, the activated carbon samples were washed with distilled water to neutral pH and dried in an oven at 50 ± 2 °C for 16 h. Dried AC was subsequently milled to the powder state (particle size ≤ 200 μm).

Burn-off values (*BO*, %) for ACs were determined as following

$$BO = \frac{wt_0 - wt}{wt_0} \cdot 100\% \quad (1)$$

where *wt*₀ and *wt* – respectively the initial weight of the dry hydrochar and the final weight of activated carbon, g.

Preparation of electrodes

The electrodes were prepared by the phase inversion method, immersion precipitation, using activated carbon as the active material and cellulose as the electrode binder (Mulder, 1996). The procedure of the electrode preparation was described in detail in the previous paper (Murashko et al., 2017). On the whole, the cellulose was ground in the planetary ball-mill and dissolved in the ionic liquid under vigorous stirring at 90 °C for 12 h to produce a 6 wt% casting solution. Respective amount of obtained activated carbon was mixed with the ionic liquid and the dispersion was placed under an ultrasound homogenizer Bandelin UW 2200 for 10 min to prevent possible formation of carbon particle agglomerates. The hot cellulose solution was added to the activated carbon dispersion and the obtained slurry with cellulose/activated carbon ratio of 1/6 was mixed by ultrasound for 5 min to ensure a homogeneous particle distribution. The casting solution was then distributed on a glass plate with an adjustable casting knife

(BYK Additives & Instruments) using an automatic film applicator BYK Additives & Instruments at room temperature. The casting thickness for all samples was 250 μm and the casting speed was 50 mm s^{-1} . All prepared materials were immersed in a deionized water coagulation bath at room temperature for 24 h. The electrodes were denoted according to the HTC conditions – AC- t - r_{HTC} .

Analytical methods

The moisture content of both hydrochar samples and activated carbons was measured with the moisture analyser balance Sartorius 7093. The morphology of the activated carbon samples was examined by Scanning Electron Microscopy (SEM) using a Hitachi SU3500 microscope. The characterization of porous carbons was carried out by nitrogen adsorption–desorption isotherms measured at 77 K using a Gemini VII Micromeritics instrument. Prior to gas adsorption measurement, the carbon samples were degassed at 300 $^{\circ}\text{C}$ under nitrogen for 3 h. BET surface area was calculated from N_2 adsorption isotherms by using the Brunauer–Emmett–Teller (BET) equation. The relative pressure range applied for the hydrochar samples was $p/p_0 = 0.05\text{--}0.25$ and for the activated carbons – $p/p_0 = 0.01\text{--}0.15$. More narrow and lower pressure region in case of activated carbons is required due to limitations of applying BET equation: only linear and continuously increasing portion of the BET plot can be used for the calculations, and in case of microporous materials this usually appear to be at the low relative pressures where the monolayer formation occurs (Rouquerol et al., 2007; De Lange et al., 2014). The total pore volume was determined from experimental isotherm by calculating the amount of nitrogen adsorbed at a relative pressure of 0.99.

The electrochemical tests were performed by using a Swagelok-type cell (Fig. 1). Two flexible self-standing electrodes were prepared from the derived cellulose composite material and dipped into 1 M H_2SO_4 ($\text{H}_2\text{SO}_4/\text{H}_2\text{O}$) electrolyte before placing into the Swagelok-type cell. The electrodes were clamped between two graphite current collectors and a cellulosic separator. The pressure between the current collectors was adjusted by screws with butterfly nuts. The Swagelok-type cell was connected to a potentiostat/galvanostat (Gamry Reference 3000), which was used for the measurement of cyclic voltammetry (CV) curves and electrochemical impedance spectroscopy (EIS) measurements.

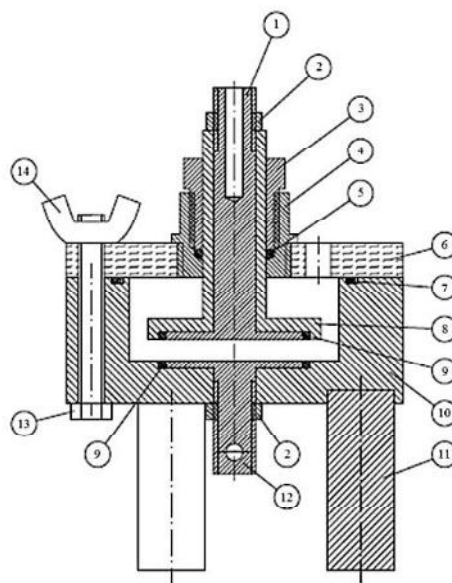


Figure 1. Swagelok-type cell used in measurements. Graphite current collectors are used due to their good chemical compatibility: 1) current collector; 2) nut; 3) seal tightening nut; 4) stud; 5) O-ring; 6) cover; 7) O-ring; 8) current collector insulation; 9) seal; 10) test chamber; 11) feet; 12) current collector; 13) screw; 14) butterfly nut.

RESULTS AND DISCUSSION

Mass yields of carbonization and activation processes

During HTC process, the solid feedstock undergoes several complex processes, which essentially modify its physical and chemical properties. Reactions of dehydration, decarboxylation with additional polymerization and aromatization are the major mechanisms of the material decomposition (Funke & Ziegler, 2010). Physical changes in the cellulose during hydrothermal carbonization lead to significant mass loss. The hydrochar mass yield (ratio between the hydrochar weight and the initial weight of feedstock on dry basis) depends on the reaction conditions (with temperature as a dominating factor) and feedstock structural properties. In the current paper, the mass yield values are in rather narrow range: 44% (HTC-2-3/1), 38% (HTC-2-6/1), 40% (HTC-4-3/1) and 36% (HTC-4-6/1). The results are consistent with data available in the literature for the hydrothermal treatment of cellulose. Sevilla & Fuertes (2009) reported the cellulose hydrochar mass yield values from 34% (at 250 °C, 2 h, 25/1 ratio) to 44% (250 °C, 2 h, 6/1 ratio) and 42.7% (250 °C, 2 h, 3/1 ratio). Reza et al. (2015) measured the product yields from 38% (250 °C, 20 min, 9/1) to 44.3% (250 °C, 8 h, 3/1). Slightly higher mass yields were reported by Diakite et al. (2013) 46.3–48.5% (230 °C, 2, 6 and 10 h, 10/1) and by Kang et al. (2012) from 48% (265 °C, 20 h, 3/1) to 53% (225 °C, 20 h, 3/1).

During chemical activation, the activation agent acts as a dehydration agent intensifying the pyrolytic decomposition of carbonaceous feedstock leading to further mass loss with simultaneous porosity development (Viswanathan et al., 2009). In current work, the burn-off of the activated carbon was on the average level of 62% for all testing runs. Sevilla et al. (2011) reported similar values of the product yield for cellulose activation with KOH at 700 °C: 34% (1/4 ratio of hydrochar/KOH) and 48% (1/2 ratio of hydrochar/KOH) which correspond to the burn-off values of 66% and 52%.

Structural properties of hydrochar samples and activated carbons

The morphology of the cellulose derived hydrochars and the obtained activated carbons is shown in Fig. 2. The figure illustrates the effect of cellulose concentration in the mixture with water during HTC process. It can be noted that hydrothermal carbonization with lower feedstock concentration (HTC-2-6/1) leads to the formation of smaller diameter spherical agglomerates (Fig. 2, b). While quite many microspheres of approx. $\text{\O}10\ \mu\text{m}$ are formed on the surface of the cellulose hydrochar HTC-2-3/1 with higher cellulose concentration (Fig. 2, a). The microspherical particles on the hydrochar resulted from the cellulose depolymerization and hydrolysis (Kang et al., 2012). Falco et al. (2011) noticed the similar formation of the spherical agglomerates during glucose carbonization, however with the higher level of homogeneity. It was noted by Kang et al. (2012) that the amount of microspheres increases with process severity (higher reaction temperature and longer reaction time). In another work by Sevilla & Fuertes (2009), an abrupt morphological change in the cellulose structure during the hydrothermal treatment was noted at the temperature around 220 °C: cellulose treatment at this temperature increases the solubility of cellulose and significantly decreases its crystallinity. The following reactions are taking place during the hydrothermal carbonization of cellulose according to their study: (i) hydrolysis of the feedstock, (ii) dehydration and fragmentation into soluble products of the monomers from the hydrolysis, (iii) polymerization or condensation of the soluble products, (iv) aromatization of the

polymers, (v) appearance of a short burst of nucleation and (vi) growth of the nuclei. It was also mentioned that high functionalization of the hydrochar makes this material an excellent precursor for the activation carbon production (Sevilla et al., 2011).

The morphology of the activated carbons is characterized with particularly irregular shapes, smooth surfaces and large cavities (Figs 2, c and 2, d). The resulted structures differ significantly from the hydrochar precursors. Sevilla & Fuertes (2009) and Falco et al. (2013) reported on the similar morphology for the activated carbons produced from different lignocellulosic components regardless of the hydrochar precursor.

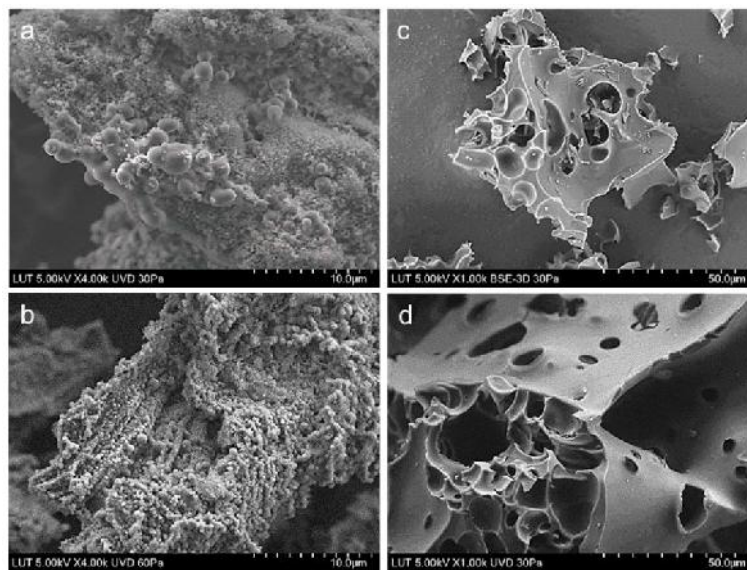


Figure 2. SEM images of the hydrochar samples before chemical activation: (a) HTC-2-3/1; (b) HTC-2-6/1. And activated carbons after chemical activation: (c) AC-2-3/1; (d) AC-2-6/1.

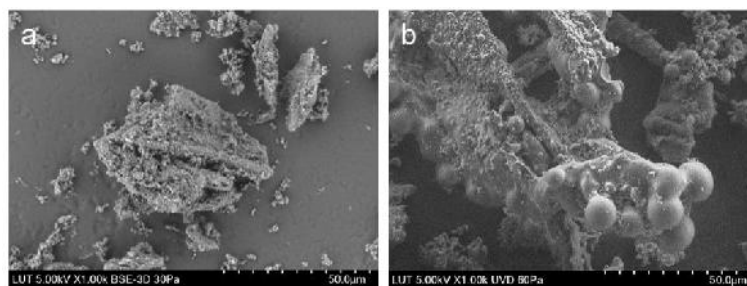


Figure 3. SEM images of the hydrochar samples HTC-2-3/1 (a) and HTC-4-3/1 (b).

Fig. 3 compares the morphology of the hydrochar samples after HTC treatment during 2 h (Fig. 3, a) and 4 h (Fig. 3, b). The carbonization structurally modifies the cellulose fibres, but they are still visible. Longer residence time results in the formation of bigger separate spheres of around $\text{\O}100 \mu\text{m}$ each. This can be the result of the secondary reactions that can occur with higher intensity of HTC treatment.

Porous textural characteristics of hydrochar samples activated carbons

During the carbonization step (e.g., HTC), the lignocellulosic components release oxygen, hydrogen and nitrogen in liquid or gaseous form and are converted into coal-like material enriched in carbon char with a rudimentary porosity (Hernández-Montoya et al., 2012; Diakite et al., 2013). Simple pyrolysis of the wood basic components in an inert atmosphere resulted in the somewhat moderate increase of the surface area: from $2.5 \text{ m}^2 \text{ g}^{-1}$ for a virgin cellulose to $394 \text{ m}^2 \text{ g}^{-1}$ for the cellulose after pyrolysis ($700 \text{ }^\circ\text{C}$, 1 h , $3 \text{ }^\circ\text{C min}^{-1}$ heating rate) (Khezami et al., 2005). The final elemental composition as well as the developed surface area of carbonized cellulose strongly depends on such parameters as heating rate, reaction temperature and residence time (Khezami et al., 2005). In general, the surface area of the hydrochars from cellulose reported in the literature is on the level of ca. $30 \text{ m}^2 \text{ g}^{-1}$ which corresponds relatively well with the external surface area (Sevilla & Fuertes, 2009). Table 1 presents the values of the BET surface area for hydrothermally carbonized materials from cellulose found in the literature and compared with the results of the current work. Although the values from the current study are in rather narrow range, the effect of HTC intensification (longer residence time and higher amount of water in the mixture) on the product porosity can be still noticed. An effect of the higher water-to-cellulose ratio can be due to the greater effect of water in the hydrolysis reaction during HTC treatment (Román et al., 2012). At the same time, the results confirm that the hydrochar samples has only rudimentary porosity before the activation step.

Table 1. BET surface areas of the cellulose derived hydrochars

Feedstock	Conditions			BET [$\text{m}^2 \text{ g}^{-1}$]	Source
	T [$^\circ\text{C}$]	t [h]	r_{HTC} [-]		
Microcrystalline cellulose	250	6	1/9	21	(Reza et al., 2015)
Microcrystalline cellulose	230	6	1/10	28	(Diakite et al., 2013)
Cellulose	230	6	n/r	28	(Mumme et al., 2011)
Cellulose	250	4	1/25	30	(Sevilla & Fuertes, 2009)
Cellulose	250	2	1/3	24	Current work
	250	2	1/6	26	
	250	4	1/3	25	
	250	4	1/6	27	

T – temperature; t – residence time; r_{HTC} – cellulose/water weight ratio; n/r – not reported.

During chemical activation with KOH, all hydrothermally carbonized cellulose samples are converted into porous carbons with high surface areas in the range of $2,300\text{--}2,645 \text{ m}^2 \text{ g}^{-1}$. Results obtained in the present study are compared with data available in the literature (Table 2). The most advanced development of porous structure is found for the sample AC-2-6/1. As compared to the initial surface area after HTC, the surface area increases tenfold after the activation.

The total pore volume is also the highest among the studied samples – $1.6 \text{ cm}^3 \text{ g}^{-1}$, while other AC samples have slightly lower values: $1.3 \text{ cm}^3 \text{ g}^{-1}$ (AC-2-3/1), $1.4 \text{ cm}^3 \text{ g}^{-1}$ (AC-4-3/1) and $1.5 \text{ cm}^3 \text{ g}^{-1}$ (AC-4-6/1). In overall, the obtained values are consistent with the values from other investigators. In the majority of the chemical activation tests with KOH, the temperature was on the level $700\text{--}800 \text{ }^\circ\text{C}$ with residence time of 1 h , generally. The impregnation ratio of KOH/char varies in the range of $0.25\text{--}4$ in the

considered literature. As a rule, the use of simple pyrolysis for char preparation results in lower values of porosity in comparison with HTC treatment (with the exception for the tests by Fujishige et al. (2017)).

Table 2. BET surface areas of the cellulose derived activated carbons

Carbonization Process conditions	Activation				BET [m ² g ⁻¹]	Source
	Activation agent	T [°C]	t [h]	r _{imp} [-]		
Pyrolysis (N ₂ , 300 °C)	KOH	700	1	0.25	678	(Khezami et al., 2005)
Pyrolysis (Ar, 600 °C)	steam	850	0.5	n/a	1,044	(Babel, 2004)
Slow pyrolysis (N ₂ , 400 °C) + fast pyrolysis (N ₂ , 900 °C)	steam	800	n/r*	n/a	1,317	(Lorenc-Grabowska & Rutkowski, 2014)
HTC	KOH	700	1	2	1,283	(Sevilla, Fuertes & Mokaya, 2011)
(250 °C, 2 h, 1/3 ratio)	KOH	800	1	4	2,047	
	KOH	700	1	4	2,370	
HTC (240 °C, 2 h, 1/10 ratio)	KOH	750	2	3	2,250	(Falco et al., 2013)
HTC (250 °C, 2 h, 1/3 ratio)	KOH	700	1	4	2,457	(Wei et al., 2011)
	KOH	800	1	4	2,125	
Pyrolysis (Ar, 600 °C)	NaOH	720	n/r	2.5	2,366	(Fujishige et al., 2017)
HTC (250 °C, 2 h, 1/3 ratio)	KOH	700	1	4	2,296	Current work
HTC (250 °C, 2 h, 1/6 ratio)	KOH	700	1	4	2,645	
HTC (250 °C, 4 h, 1/3 ratio)	KOH	700	1	4	2,494	
HTC (250 °C, 4 h, 1/6 ratio)	KOH	700	1	4	2,580	

* to 50% burn-off; T – temperature; t – residence time; r_{imp} – KOH/cellulose weight ratio; n/r – not reported; n/a – not applicable.

Electrochemical tests

The results of the electrochemical analysis of the prepared samples are presented in Fig. 4. The specific capacitance of the samples (Fig. 4, a) was measured with 50 mV s⁻¹ scan rate and the obtained values are given in Table 3. Additionally, the different values of the scan rates were applied to evaluate the capacity retention of the prepared electrodes (Fig. 4, b).

As it can be seen in Fig. 4, a, the effect of residence time during HTC on the electrodes performance is more pronounced than the effect of feedstock concentration within the studied reaction parameters. The electrodes produced from the samples carbonized during 2 h (AC-2-3/1 and AC-2-6/1) show comparable performance and have higher specific capacitances than other two samples carbonized during 4 h. The sample AC-2-3/1 reveals the highest value of the specific capacitance in spite of the fact that it has not the highest BET surface area among others. As one of the possible reasons for such results, the nanopores of the prepared AC are not fully used during the creation of the electrochemical double layer, where the charge is stored.

The variations of capacity retention within different scan rates show relatively similar results for all samples. However, the capacity retention is slightly higher for the samples AC-4-3/1 and AC-4-6/1 than for the samples AC-2-3/1 and AC-2-6/1. The obtained results may be explained by the influence of the secondary reaction products during the carbonization process that may have an influence on the final product characteristics. With higher severity of the carbonization process, the additional chemical reactions occur during the HTC process. If the products of those reactions were not fully removed from the material, the purity of the final product is decreased, which in its turn leads to the decreasing of the electrochemical properties of the prepared material (by increasing the material resistance). The trace metals and salts (e.g., Ca and Mg salts) that originally containing in the cellulose may have an impact on the properties of the final product.

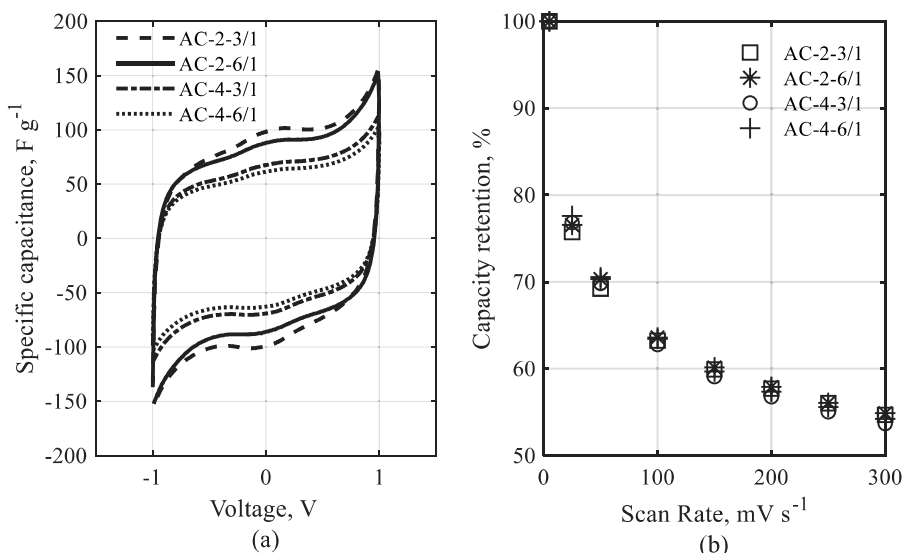


Figure 4. Specific capacitance (a) and capacity retention (b) of the created EDLCs from prepared composite materials.

Table 3. Specific capacitance of the studied samples at 50 mV s⁻¹ scan rate

Samples	AC-2-3/1	AC-2-6/1	AC-4-3/1	AC-4-6/1
Specific capacitance, F g ⁻¹	110.3	102.5	77.2	69.4

The similar result was obtained from the impedance analysis of the prepared samples, which is shown in Fig. 5. The samples AC-4-3/1 and AC-4-6/1 have higher value of the impedance at low operation frequency than samples AC-2-3/1 and AC-2-6/1. Similarly to the explanation above, the products of the side reactions may influence on the diffusion of electrolyte ions into the pores of electrode materials which may lead to the increase of the impedance values for the prepared electrodes. Therefore, with purpose to improve the quality of the produced AC an additional purification of the material, prepared by using a long residence time during hydrothermal carbonization, may be necessary.

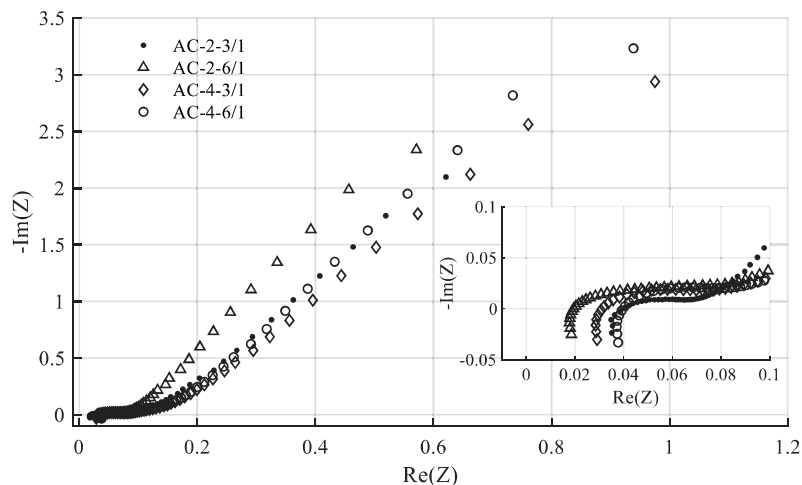


Figure 5. Impedance of the created EDLCs from prepared composite materials.

CONCLUSIONS

Porous activated carbons were produced from cellulose-derived hydrochars with KOH chemical activation. The presented results proved that cellulose can be successfully used as a feedstock for electrodes of electrical double layer capacitors. The possibility to tune the porosity of activated carbons is essential for various application. Several variations of reaction conditions during the hydrothermal carbonization were tested in order to evaluate the influence of hydrochar preparation on the characteristics of the final product. This work demonstrates that not only the HTC reaction temperature but also the ratio between the feedstock and water and the residence time have certain effect on the porosity development of the final product. The significance of these reaction parameters is generally underestimated and their effect is not well studied. The increase of the process severity (longer reaction time and higher amount of water in water-cellulose mixture) increases the surface area of the derived hydrochar samples. Within the frames of the studied reaction parameters, the sample HTC-4-6/1 after the HTC treatment during 4 h and with water/cellulose ratio of 6/1 have the highest BET surface area of $27 \text{ m}^2 \text{ g}^{-1}$. Chemical activation allows to convert the hydrochar samples into porous activated carbons with high surface areas in the range of $2,300\text{--}2,645 \text{ m}^2 \text{ g}^{-1}$. The highest surface areas of activated carbons were found for the samples produced from the cellulose hydrochars after 2 and 4 h with water/cellulose ratio of 6/1.

The flexible self-standing electrodes for an electrical double layer capacitors were successfully produced and their electrochemical characteristics were analysed. Even though all studied samples show rather comparable values for the capacity retention, the levels of specific capacity differ significantly for the samples after different reaction times. Despite the fact that the samples AC-4-3/1 and AC-4-6/1 have the higher BET surface areas than samples produced during 2 h of HTC, the highest specific capacitances are found for AC-2-3/1 and AC-2-6/1: 110.3 and 102.5 F g^{-1} correspondingly. That can be possibly explained by non-complete use of the developed nanopores of the activated carbon during the creation of the electrochemical double layer. Moreover, the samples

AC-4-3/1 and AC-4-6/1 have the higher value of the impedance at low operation frequency than samples AC-2-3/1 and AC-2-6/1. The products of the secondary reactions during HTC may influence on the diffusion of electrolyte ions into the pores of electrode materials that may lead to such results.

The obtained results prove that HTC in combination with chemical activation may be effectively used to convert the feedstock material into highly porous activated carbon. Higher intensity of the HTC process (longer residence time and higher water-to-feedstock ratio) leads to more severe decomposition of the initial material and, as a consequence, higher porosity. At the same time, more research is required to determine accurate correlations between the reaction parameters and final characteristics of the product. Possible side effects during longer time of reaction should be thoroughly studied with wider variation of the process parameters. Moreover, the possibility to use some organic by-products and wastes instead of pure cellulose would be extremely beneficial for future research.

ACKNOWLEDGEMENTS. The authors would like to thank Toni Väkiparta and Liisa Puro from Chemical Technology Unit of LUT University for valuable help and assistance during the analysis of the samples.

REFERENCES

- Babel, K. 2004. Porous structure evolution of cellulose carbon fibres during heating in the initial activation stage. *Fuel Processing Technology* **85**(1), 75–89.
- Babel, S. & Kurniawan, T.A. 2003. Low-cost adsorbents for heavy metals uptake from contaminated water: a review. *Journal of Hazardous Materials* **97**(3), 219–243.
- Cao, J., Zhu, C., Aoki, Y. & Habazaki, H. 2018. Starch-Derived Hierarchical Porous Carbon with Controlled Porosity for High Performance Supercapacitors. *ACS Sustainable Chemistry & Engineering* **6**(6), 7292–7303.
- Crini, G. 2006. Non-conventional low-cost adsorbents for dye removal: A review. *Bioresource Technology* **97**(9), 1061–1085.
- da Silva Lacerda, V., Lopez-Sotelo, J.B., Correa-Guimaraes, A., Hernandez-Navarro, S., Sanchez-Bascones, M., Navas-Gracia, L. M. & Martin-Gil, J. 2015. Rhodamine B removal with activated carbons obtained from lignocellulosic waste. *Journal of Environmental Management* **155**, 67–76.
- De Lange, M.F., Vlugt, T. J.H., Gascon, J. & Kapteijn, F. 2014. Adsorptive characterization of porous solids: Error analysis guides the way. *Microporous and Mesoporous Materials* **200**, 199–215.
- Deng, L., Young, R.J., Kinloch, I.A., Abdelkader, A.M., Holmes, S.M., De Haro-Del Rio, D.A. & Eichhorn, S.J. 2013. Supercapacitance from cellulose and carbon nanotube nanocomposite fibers. *ACS Applied Materials and Interfaces* **5**(20), 9983–9990.
- Diakite, M., Paul, A., Jäger, C., Pielert, J. & Mumme, J. 2013. Chemical and morphological changes in hydrochars derived from microcrystalline cellulose and investigated by chromatographic, spectroscopic and adsorption techniques. *Bioresource Technology* **150**, 98–105.
- Falco, C., Baccile, N. & Titirici, M.-M. 2011. Morphological and structural differences between glucose, cellulose and lignocellulosic biomass derived hydrothermal carbons. *Green Chemistry* **13**(11), 3273.
- Falco, C., Marco-Lozar, J.P., Salinas-Torres, D., Morallón, E., Cazorla-Amorós, D., Titirici, M.M. & Lozano-Castelló, D. 2013. Tailoring the porosity of chemically activated hydrothermal carbons: Influence of the precursor and hydrothermal carbonization temperature. *Carbon* **62**, 346–355.

- Fujishige, M., Yoshida, I., Toya, Y., Banba, Y., Oshida, K., Tanaka, Y., Dulyaseree P., Wongwiriyan, W. & Takeuchi, K. 2017. Preparation of activated carbon from bamboo-cellulose fiber and its use for EDLC electrode material. *Journal of Environmental Chemical Engineering* **5**(2), 1801–1808.
- Funke, A. & Ziegler, F. 2010. Hydrothermal carbonization of biomass: A summary and discussion of chemical mechanisms for process engineering. *Biofuels, Bioproducts and Biorefining* **4**(2), 160–177.
- Hartmann, S., Iurchenkova, A., Kallio, T. & Fedorovskaya, E. 2020. Electrochemical Properties of Nitrogen and Oxygen Doped Reduced Graphene Oxide. *Energies* **13**(2), 312.
- Hernández-Montoya, V., García-Servín, J. & Bueno-López, J.I. 2012. Thermal Treatments and Activation Procedures Used in the Preparation of Activated Carbons. Lignocellulosic Precursors Used in the Synthesis of Activated Carbon - Characterization Techniques and Applications in the Wastewater Treatment, Chapter 2, pp. 19–36.
- Jiang, Z., Liu, Y., Sun, X., Tian, F., Sun, F., Liang, C., You, W., Han, C. & Li, C. 2003. Activated carbons chemically modified by concentrated H₂SO₄ for the adsorption of the pollutants from wastewater and the dibenzothiophene from fuel oils. *Langmuir* **19**(3), 731–736.
- Kang, S., Li, X., Fan, J. & Chang, J. 2012. Characterization of hydrochars produced by hydrothermal carbonization of lignin, cellulose, d-xylose, and wood meal. *Industrial and Engineering Chemistry Research* **51**(26), 9023–9031.
- Kim, H., Shin, J., Jang, I. & Ju, Y. 2019. Hydrothermal Synthesis of Three-Dimensional Perovskite NiMnO₃ Oxide and Application in Supercapacitor Electrode. *Energies* **13**(1), 36.
- Khezami, L., Chetouani, A., Taouk, B. & Capart, R. 2005. Production and characterisation of activated carbon from wood components in powder: Cellulose, lignin, xylan. *Powder Technology* **157**(1), 48–56.
- Kuzmenko, V., Naboka, O., Haque, M., Staaf, H., Göransson, G., Gatenholm, P. & Enoksson, P. 2015. Sustainable carbon nanofibers/nanotubes composites from cellulose as electrodes for supercapacitors. *Energy*, **90**, Part 2, 1490–1496.
- Lee, K.K., Hao, W., Gustafsson, M., Tai, C.-W., Morin, D., Björkman, E., Lilliestråle, M., Björefors, F., Andersson, A.M. & Hedin, N. 2016. Tailored activated carbons for supercapacitors derived from hydrothermally carbonized sugars by chemical activation. *RSC Advances* **6**(112), 110629–110641.
- Li, Z., Yi, W., Li, Z., Tian, C., Fu, P., Zhang, Y. & Teng, J. 2020. Preparation of Solid Fuel Hydrochar over Hydrothermal Carbonization of Red Jujube Branch. *Energies* **13**(2), 480.
- Lorenc-Grabowska, E. & Rutkowski, P. 2014. High basicity adsorbents from solid residue of cellulose and synthetic polymer co-pyrolysis for phenol removal: Kinetics and mechanism. *Applied Surface Science* **316**(1), 435–442.
- Lozano-Castelló, D., Lillo-Ródenas, M.A., Cazorla-Amorós, D. & Linares-Solano, A. 2001. Preparation of activated carbons from Spanish anthracite - I. Activation by KOH. *Carbon* **39**(5), 741–749.
- Mesfun, S., Matsakas, L., Rova, U. & Christakopoulos, P. 2019. Technoeconomic Assessment of Hybrid Organosolv–Steam Explosion Pretreatment of Woody Biomass. *Energies* **12**(21), 4206.
- Mohamad, N., Lau, L.C., Lee, K. T. & Mohamed, A.R. 2013. Synthesis of activated carbon from lignocellulosic biomass and its applications in air pollution control—a review. *Journal of Environmental Chemical Engineering* **1**(4), 658–666.
- Mohan, D. & Pittman Jr., C.U. 2007. Arsenic removal from water/wastewater using adsorbents—A critical review. *Journal of Hazardous Materials* **142**(1), 1–53.
- Mulder, M. 1996. Preparation of Synthetic Membranes. In *Basic Principles of Membrane Technology*. Springer, Netherlands, pp. 71–156.
- Mumme, J., Eckervogt, L., Pielert, J., Diakité, M., Rupp, F. & Kern, J. 2011. Hydrothermal carbonization of anaerobically digested maize silage. *Bioresource Technology* **102**(19), 9255–9260.

- Murashko, K., Nevstrueva, D., Pihlajamaki, A., Koiranen, T. & Pyrhonen, J. 2017. Cellulose and activated carbon based flexible electrical double-layer capacitor electrode: Preparation and characterization. *Energy* **119**, 435–441.
- Pandolfo, A.G. & Hollenkamp, A.F. 2006. Carbon properties and their role in supercapacitors. *Journal of Power Sources* **157**(1), 11–27.
- Rengaraj, S., Moon, S.-H., Sivabalan, R., Arabindoo, B. & Murugesan, V. 2002. Agricultural solid waste for the removal of organics: adsorption of phenol from water and wastewater by palm seed coat activated carbon. *Waste Management* **22**(5), 543–548.
- Reza, M.T., Rottler, E., Tölle, R., Werner, M., Ramm, P. & Mumme, J. 2015. Production, characterization, and biogas application of magnetic hydrochar from cellulose. *Bioresource Technology* **186**, 34–43.
- Román, S., Nabais, J.M.V., Laginhas, C., Ledesma, B. & González, J.F. 2012. Hydrothermal carbonization as an effective way of densifying the energy content of biomass. *Fuel Processing Technology* **103**, 78–83.
- Rouquerol, J., Llewellyn, P. & Rouquerol, F. 2007. Is the BET equation applicable to microporous adsorbents? *Studies in Surface Science and Catalysis* **160**, 49–56.
- Saha, D., Li, Y., Bi, Z., Chen, J., Keum, J., Hensley, D. & Naskar, A. 2014. Studies on Supercapacitor Electrode Material from Activated Lignin-Derived Mesoporous Carbon. *Langmuir* **30**(3), 900–910.
- Sevilla, M. & Fuertes, A.B. 2009. The production of carbon materials by hydrothermal carbonization of cellulose. *Carbon* **47**(9), 2281–2289.
- Sevilla, M., Fuertes, A.B. & Mokaya, R. 2011. High density hydrogen storage in superactivated carbons from hydrothermally carbonized renewable organic materials. *Energy & Environmental Science* **4**(4), 1400–1410.
- Sun, Y., Wang, Z., Liu, Y., Meng, X., Qu, J., Liu, C. & Qu, B. 2019. A Review on the Transformation of Furfural Residue for Value-Added Products. *Energies* **13**(1), 21.
- Titirici, M.M., Thomas, A., Yu, S.-H., Müller, J.-O. & Antonietti, M. 2007. A direct synthesis of mesoporous carbons with bicontinuous pore morphology from crude plant material by hydrothermal carbonization. *Chemistry of Materials* **19**(17), 4205–4212.
- Titirici, M.-M. & Antonietti, M. 2010. Chemistry and materials options of sustainable carbon materials made by hydrothermal carbonization. *Chemical Society Reviews* **39**(1), 103–116.
- Viswanathan, B., Neel, P. & Varadarajan, T. 2009. Methods of activation and specific applications of carbon materials. *Methods of Activation and Specific Applications of Carbon Materials*, pp. 16–17.
- Wang, Z., Tammela, P., Strømme, M. & Nyholm, L. 2017. Cellulose-based Supercapacitors: Material and Performance Considerations. *Advanced Energy Materials* **7**(18).
- Wei, L., Sevilla, M., Fuertes, A.B., Mokaya, R. & Yushin, G. 2011. Hydrothermal carbonization of abundant renewable natural organic chemicals for high-performance supercapacitor electrodes. *Advanced Energy Materials* **1**(3), 356–361.
- Yuan, M., Que, H., Yang, X. & Li, M. 2019. Nitrogen and oxygen co-doped glucose-based carbon materials with enhanced electrochemical performances as supercapacitors. *Ionic* **25**(9), 4305–4314.
- Zhang, K., Liu, M., Zhang, T., Min, X., Wang, Z., Chaiab, L. & Shi, Y. 2019. High-performance supercapacitor energy storage using a carbon material derived from lignin by bacterial activation before carbonization. *Journal of Materials Chemistry A* **7**(47), 26838–26848.
- Zhu, Y., Murali, S., Stoller, M.D., Ganesh, K.J., Cai, W., Ferreira, P.J. & Ruoff, R.S. 2011. Carbon-based supercapacitors produced by activation of graphene. *Science* **332**(6037), 1537–1541.